

SUSCEPTIBILITY OF LOW STRENGTH RUTILE FLUX-CORED WELD METAL TO HYDROGEN ASSISTED COLD CRACKING



M. Pitrun¹



D. Nolan²

¹ HRL Technology, Melbourne

² University of Wollongong
(Australia)

E-mail: ¹ mpitrun@hrl.com.au

² dnolan@uow.edu.au

ABSTRACT

This paper presents the results of an investigation into hydrogen assisted cold cracking (HACC) susceptibility of seamless and seamed low strength rutile flux cored wires, with nominal diffusible hydrogen (H_D) levels of 5 and 10 ml/100 g, respectively. The objective was to assess the influence of key welding parameters on susceptibility of weld metal to cold cracking. Parameters investigated were the welding current, the contact-tip to work-piece distance (CTWD), the shielding gas and the preheat temperature. The gapped bead-on-plate (G-BOP) test was used to examine the effects of these parameters on the extent of weld metal transverse cracking at a range of preheat temperatures. The overall results indicate that the weld metal susceptibility to cold cracking correlates with diffusible hydrogen content, H_D . It was found that, without preheat, the seamless wire weld deposits (< 5 ml/100 g) did not crack, whereas all those weld metals produced using the seamed wire (> 5 ml/100 g) exhibited cold cracking. Weld metal deposited using 75Ar-25CO₂ shielding gas resulted in a higher H_D levels than for CO₂ shielding gas and, consequently, a higher susceptibility to cold cracking for no or low temperature preheat conditions. Preheating was found to have a strong effect on crack susceptibility, substantially decreasing the amount of cold cracking in the seamed wire welds.

IIW-Thesaurus keywords: Cold cracking; Cracking; Defects; Hydrogen; Gases; Influencing factors; Process parameters; Process conditions; Weld metal; Current; Shielding gases; Gases; Preheating; Heat treatment; Weldability tests; Hardness; Mechanical properties; FCA welding; Arc welding; Practical investigations; Reference lists.

1 INTRODUCTION

Hydrogen assisted cold cracking (HACC) can be initiated either in the parent metal HAZ or the weld metal, wherever a sufficient amount of hydrogen is present in the welded joint, accumulated at a site of high stress concentration within a susceptible microstructure.

Traditionally, processing factors such as preheat temperature, plate thickness, selection of welding process, welding consumable strength and nominal hydrogen content, are chosen to avoid HACC in the HAZ of the parent plate, as specified in various welding standards.

Modern steels have become more resistant to HAZ hydrogen cracking as a result of reduced alloying content and the introduction of thermo-mechanically controlled processing (TMCP). The current generation of structural steels is characterized by leaner chemistry and more sophisticated thermo-mechanical processing, particularly lower carbon content and the development of strength through grain size control and micro-alloying

Doc. IIW-1723-05 (ex-doc. IX-2166-05) recommended for publication by Commission IX "Behaviour of metals subjected to welding".

with strong carbide forming elements. This reduction in the carbon and carbon equivalent levels [1] has significantly lowered the risk of hydrogen cracking in the HAZ. As a result, the focus of attention has switched to the weld metal, particularly the development of transverse weld metal cracking in thick plate welds [2]. Consequently, it is becoming increasingly important to develop reliable testing methods that provide accurate data for the development of guidelines for the avoidance of weld metal hydrogen cracking.

Although there are guidelines and welding standards for avoidance of HACC in the HAZ [3-6], a universal and reliable model for HACC avoidance in the weld metal is expected to be more complex and difficult than for hydrogen cracking in parent metal [7]. Therefore, independent management procedures for avoiding HACC in the weld metal are yet to be developed.

In general, the susceptibility of weld metal to hydrogen cracking appears to increase with an increase in weld metal strength, hydrogen content and section thickness increase [7, 8] and is more complex than the case of HAZ cracking [9]. Weld metal hydrogen cracking in transverse direction has been reported in a thick multi-pass weld FCAW welds using a high strength [10] and low strength [11] rutile flux cored wires. Interestingly, no cracking was observed in the HAZ in either work.

The aim of the investigation reported in this paper was to analyse G-BOP test results for the FCAW process in the light of information previously reported on the effects of welding parameters on hydrogen content in the weld metal generated by the flux cored wires [12]. The examination of two low strength rutile wires of the same classification, but different nominal hydrogen levels, has provided an opportunity to evaluate the role of hydrogen on crack susceptibility in low strength weld metal.

2 WELDABILITY TESTS

The first test methods for cold cracking emerged in the 1940s [13], when the formation of martensite in the HAZ was the main cause of cracking. Following World War II, there was progressive development of hydrogen-induced cracking tests for a range of weld configurations and applications. These tests became gradually more sophisticated, and some were designed specifically for the investigation of the mechanism of HACC and for the proper selection of welding conditions for its avoidance during welding fabrication. Historically, most of the methods were designed to simulate some particular application in which cracking was experienced. The main objective of weldability tests is to examine the effects of various factors on cracking susceptibility, including parent metal composition, type of welding consumable, pre-heat temperature and other welding conditions. The basic idea of all testing methods is to obtain a reliable and representative indication of crack susceptibility in relation to a defined set of test criteria. Cold cracking tests are used to:

- examine sensitivity to welding variables and other surrounding conditions that effect hydrogen cracking,
- examine the relationship between welding consumable and parent metal,
- provide a preliminary examination of the cracking mechanism, and
- establish welding conditions that avoid or minimise hydrogen cracking for a particular combination of welding process, consumable and parent metal.

In view of the crack location, testing methods for susceptibility to HACC are divided into two groups, those that study HACC in the HAZ or in the weld metal. Although the earlier tests were developed primarily to measure susceptibility to HAZ cracking, several tests have been designed specifically for weld metal cracking, or both as shown in Table 1.

Table 1 – A listing of the various testing methods for determining hydrogen cracking in parent metal HAZ and weld metal

| TEST | Mode of Cracking Imposed | | |
|--|--------------------------|------------|-----------|
| | HAZ | Weld Metal | Weld Pass |
| Reeve restraint cracking | x | | S |
| Non-restraint fillet | x | | S |
| Tekken (Y groove) | x | | S |
| Controlled thermal severity (CTS) | x | | S |
| Implant | x | | S |
| Tensile restraint cracking (TRC) | x | | S |
| Rigid restraint cracking (RRC) | x | | S/M |
| H slit restraint cracking | x | | S/M |
| Cruciform | x | | M |
| Cranfield | x | | M |
| Lehigh (U groove) restraint cracking | x | x | S |
| Lehigh (slot groove) restraint cracking | x | x | S |
| Welding Institute of Canada (WIC) | x | x | S |
| Circular patch (BWRA) | x | x | M |
| Longitudinal bead – tensile restraint (LB-TRC) | | x | S |
| Longitudinal restraint cracking | | x | S |
| V groove weld | | x | M |
| Gapped bead on plate (G-BOP) | | x | S/M |
| Note: S = single, M = multiple. | | | |

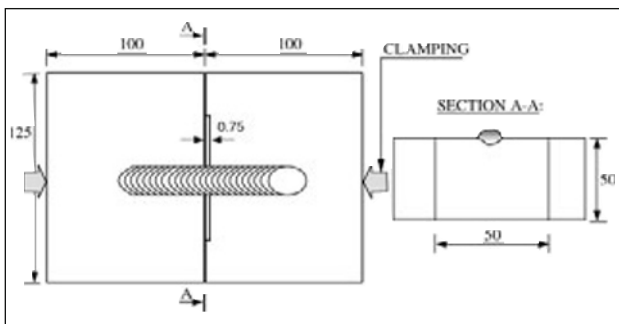
The majority of these tests were designed as small scale laboratory tests, using a single weld pass. Other, more expensive weldability tests were designed for multi-pass welds that take into account the interacting effects of thermal cycles, changes of thermal stresses, and increase in restraint associated with progress of welding through the plate thickness. A number of studies have comprehensively reviewed the most commonly used weldability testing methods for HACC and weld metal [9, 14-16]. Although there are fundamental differ-

ences between the testing methods, particularly in terms of the different levels of restraint imposed, a number of cracking tests have proven to be sufficiently reliable that they have been accepted in American [17], British [18], French [19] and Japanese [20] standards. The Lehigh, CTS, G-BOP, Implant and Tekken tests are the most widely adopted tests.

The G-BOP Test

Transverse cracking can occur when welding over a small gap that acts as a stress concentrator. This situation can arise for poor fit up in highly restraint joints. In the early 1960s, The Brown-Boveri test was introduced to examine cracking sensitivity. This test was initially designed for austenitic steels and the sample consisted of several machined thick plates bolted together [21]. During the early 1970s, the E.O. Paton Welding Institute designed a test piece with an artificial notch that enabled initiation of a cold crack in a transverse direction to the weld [22]. Following this concept, the effect of a self-restraint gapped bead-on-plate test (G-BOP) was established [23], in which a gap underneath the weld introduces a large stress concentration assisting initiation of transverse weld metal cracking.

Early work on the G-BOP test by Graville and McParlan [23], showed that the test was suitable for the determination of cold cracking susceptibility as a function of preheat temperature. The results indicated that by increasing preheat temperature, cracking was gradually suppressed. The mechanism of cold cracking was also elucidated through measurement of the stress level variation across the gap. The G-BOP test sample consists of two 50 mm thick steel blocks, one of which has a machined 0.75 mm deep recess. The blocks are clamped together to prevent any relative movement, and a bead is deposited along the top surface over the gap, as shown in Figure 1.



Note: All dimensions in millimetres [not to scale].

Figure 1 – A diagram of the G-BOP test configuration (after Graville and McParlan [23])

After welding, the blocks are left in clamps for a minimum of 48 hours to provide the necessary restraint and to allow hydrogen cracking to develop. The welds are then heated to a dull red heat in the vicinity of the gap to allow heat tinting of the fracture surfaces. The samples are then allowed to cool to room temperature, and are broken open to reveal the fracture surfaces in the weld. Any cracks that

developed in the weld metal during the dwell time of 48 hours are heat tinted, revealing a dark blue or grey discoloration of the fracture surface. Any non-cracked weld metal cross-section has light grey metallic appearance.

Several researchers later modified the test [16, 24-27]. These modifications predominantly included variations of test block dimensions, incubation periods, clamping forces and releasing time of clamps. Further modification of the testing procedure allowed rotation of test blocks to deposit 4 weld beads [16]. Although the G-BOP test is primarily used to assess the susceptibility of the welding consumable to cold cracking, this method was also successfully used for a study of parent metal dilution in a weld metal [28].

In order to minimise the dilution effects, a modified G-BOP test has been developed to test the weld metal composition without the influence of dilution with parent metal. The plate is prepared by weld surfacing (buttering) with the weld metal before machining of the test piece. This technique is particularly applicable to study of hydrogen cracking in alloyed and multi-pass weld deposits [26]. The G-BOP test can be quantified by a room temperature cracking parameter (RTC), or a cracking parameter for preheat temperatures above 20 °C.

However, in the case of consumables containing higher levels of diffusible hydrogen, RTC is usually 100 %, and the parameter is inadequate [26]. Therefore, a parameter known as the 10 % crack preheat temperature (10 % CPT), defined as the preheat temperature required to limit cracking to $\leq 10\%$, was found to be more suitable [25, 26]. This parameter may be useful where two consumables produce similar amounts of diffusible hydrogen in their weld deposits and exhibit 100 % RTC, but may respond differently to an increase in preheat temperature. That is, the 10 % CPT values are different. Another useful parameter is the critical preheat temperature (CPT), obtained by extrapolation, at which the cracking percentage is expected to be $< 5\%$ [16]. The major benefit of the G-BOP test is that it can be used as a quick and inexpensive “go” or “no-go” comparative method to rank consumables with respect to susceptibility to cold cracking. The standard procedure can be also enhanced by an instrumented G-BOP test. This enhancement can be achieved by recording temperature history and cooling rates, or longitudinal stresses across the gap during the weld bead cooling [29].

The main aim of this current study was to observe the effect of preheat temperatures on susceptibility to cold cracking for a range of welding conditions in the FCAW process. Previous work by Pitrun *et al.* [12] established the levels of diffusible hydrogen in the weld bead for the same conditions and consumables, under controlled laboratory conditions.

3 EXPERIMENTAL PROCEDURE

3.1 Equipment and materials

Standard G-BOP tests were carried out using the same welding equipment as for the diffusible hydrogen testing

program previously reported [12]. A conventional 3-phase DC welding machine, Transmig 400 was used that has been widely adopted by industry for continuous gas-shielded wire processes (GMAW and FCAW). To allow full control of welding parameters, of travel speed, position of welding torch and CTWD, the welding torch was fixed onto a travelling mechanism mounted on the top of a support the frame. This enabled continuous horizontal movement under controlled conditions.

All of the G-BOP experiments were conducted using the identical spools of wire that were used in the welding trials for the previous work that determined the effect of welding parameters on diffusible hydrogen content [12]. Therefore, other than for the effects of varying atmospheric conditions (recorded for each set of test samples), the probability of significant variation in diffusible hydrogen levels between the two sets of results is low.

3.2 Welding consumables

In Australia there are two standards for carbon steel flux-cored wires that are commonly used by industry, ANSI/AWS A5.20-95 [30] and AS 2203.1-1990 [31]. However, the wire classification systems referred to in these standards and the methods of specifying nominal hydrogen levels vary significantly. The current work adopts the American ANSI/AWS A5.20-95 classification system for flux-cored consumables, rather than the more complex AS 2203.1-1990 Australian terminology. In this way, the low strength rutile consumables used in the current work are referred to as E71T-1, rather than ETP-GMp-W503A, as in AS 2203.1-1990. In addition, specification of hydrogen levels in the current work adopts the ISO 3690:2000 [32] and AS 2203.1-1990 benchmarks, with the wires further designated as H5 and H10, with nominal levels of diffusible hydrogen in deposited weld metal of 5 and 10 ml/100 g, respectively. These designations are more commonly used for hydrogen levels of FCAW consumables.

Two commercially available, seamless and seamed tubular gas shielded flux-cored wires of 1.6 mm in diameter were used in this current work. These two wire types are considered to be the most widely used for FCAW of C and C-Mn steels for all positional applications in the Australian industry. Both the seamless (H5) and seamed (H10) wires are micro-alloyed rutile

types based on a titanium-boron flux composition. The wires not only significantly differ in the nominal hydrogen levels but also in their cross-section design, as shown in Figure 3 of reference [12]. The butt seam of H10 wire was not fully closed leaving approximately 0.1 mm gap, thereby allowing the ingress of moisture or wire lubricant through the seam during the manufacturing process, or subsequent storage and use. It should also be noted that similar gaps have been also observed on equivalent wires supplied by a range of manufacturers.

The chemical compositions of “all-weld metal” deposits, carried out in accordance to the Australian standard AS 2203.1-1990, for the two wires used in the current work are presented in Table 2. While CE_{IWW} values are very similar for both the H5 and H10 wires, the Pcm values for the H10 wire samples were noticeably higher for both shielding gases used. This is due to higher levels of carbon and boron in the H10 weld metal deposits, since both carbon and boron concentration are more important factors in the Pcm carbon equivalent formula. A graphical comparison of the carbon equivalent values is presented in Figure 2. It should be noted that the CE_{IWW} and Pcm values were calculated from multiple layer “all-weld metal” deposits, and different values would be obtained from a single weld bead due to the dilution effects. Typically, the use of CO₂ shielding gas reduces Mn, Si and B recovery, and this has resulted in marginally lower CE_{IWW} and Pcm values for both consumables.

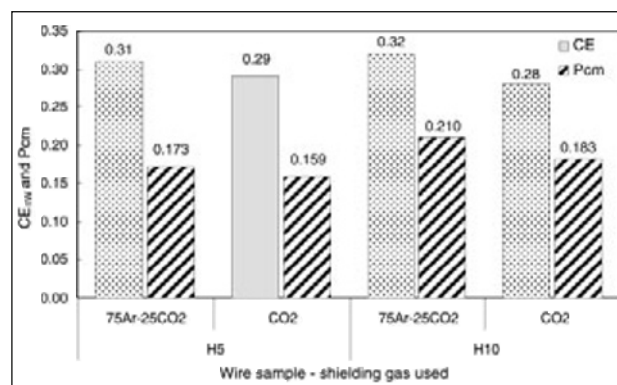


Figure 2 – Graph showing the CE_{IWW} and Pcm values for H5 and H10 “all-weld metals” deposited using 75Ar-25CO₂ and CO₂ shielding gases

Table 2 – Chemical composition (weight percentage) of all-weld metal deposits of H5 and H10 FCAW consumables, using 75Ar-25CO₂ and CO₂ shielding gas

| | All-weld metal chemical analysis of wire samples (% weight) | | | | | | | | | | | | | | | | CE _{IWW} | Pcm | |
|------------------------|---|------|------|-------|-------|-------|-------|-------|-------|-------|-------|-------|--------|-------|--------|-------|-------------------|-------|--|
| | C | Mn | Si | S | P | Ni | Cr | Mo | Cu | V | Nb | Ti | B | Al | N | O | | | |
| (H5) | | | | | | | | | | | | | | | | | | | |
| 75Ar-25CO ₂ | 0.043 | 1.46 | 0.59 | 0.009 | 0.011 | 0.051 | 0.055 | 0.008 | 0.14 | 0.014 | 0.011 | 0.044 | 0.0043 | 0.008 | 0.0084 | 0.043 | 0.31 | 0.173 | |
| CO ₂ | 0.050 | 1.25 | 0.47 | 0.010 | 0.011 | 0.052 | 0.054 | 0.008 | 0.15 | 0.013 | 0.010 | 0.042 | 0.0032 | 0.007 | 0.0097 | 0.059 | 0.29 | 0.159 | |
| (H10) | | | | | | | | | | | | | | | | | | | |
| 75Ar-25CO ₂ | 0.070 | 1.41 | 0.61 | 0.011 | 0.012 | 0.025 | 0.027 | 0.003 | 0.029 | 0.015 | 0.012 | 0.051 | 0.0090 | 0.004 | 0.0042 | 0.059 | 0.32 | 0.210 | |
| CO ₂ | 0.065 | 1.15 | 0.48 | 0.012 | 0.012 | 0.024 | 0.025 | 0.002 | 0.025 | 0.015 | 0.010 | 0.039 | 0.0077 | 0.003 | 0.0067 | 0.055 | 0.28 | 0.183 | |

3.3 G-BOP test plates

The G-BOP test samples were prepared from a 50 mm thick rolled plate made from AS 3678-1999 Grade 250 steel with a chemical composition, as shown in Table 3.

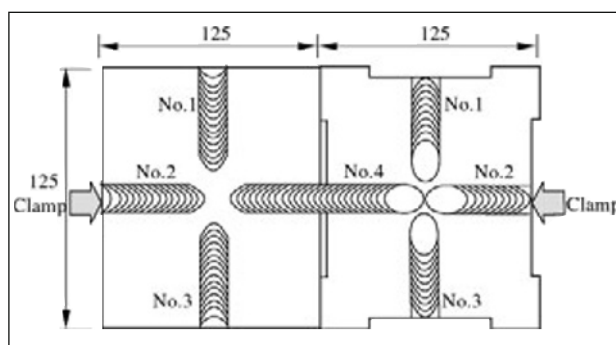
In order to avoid a variation of results caused by a possible inconsistency between different batches of wires, the entire experimental work was carried out using only one spool from each wire supplied. After completion of each experiment, the wire was re-packed into its original packaging and stored in dry conditions at ambient temperature. In this way, the effect of long time exposure of wires to varying atmospheric conditions between the experiments was kept to minimum.

3.4 Testing procedure and welding parameters

As proposed by Graville *et al.* [23], four 0.75 mm deep recesses were machined in one of the mating blocks to introduce a notch for initiation of transverse weld metal cracking. The multiple recesses enabled the use of the same pair of blocks for four weld passes, as shown in Figure 3.

The G-BOP tests were carried out on both H5 and H10 weld deposits using preheat temperatures of 20, 50, 80, 100 and 120 °C. Samples were preheated at temperature for 60 minutes and the furnace temperature was set 10 °C higher, thereby allowing for the time required to align and clamp the pair of blocks together prior to welding. Once the temperature of the blocks was stabilised at desired preheat temperature (+10 °C), the mating blocks were quickly joined together by a large G-clamp, approximately in the middle of the block thickness. In order to allow a uniform loss of heat through radiation, the assembled blocks were rested on two supporting plates positioned across the block ends.

Weld beads of 100-120 mm in length were deposited. Relative humidity and ambient temperature were recorded for each welded test block. Immediately after completion of welding, the blocks were allowed to cool down to ambient temperature in still air, while remaining restrained in the clamp for a minimum period of 72 hours. After this period of time, the restraining clamp was released, and a small area in the vicinity of the weld bead (just over the gap of the two mating halves) was heated up to a dull, cherry red colour using a gas flame and maintained for about 10 seconds. This procedure was designed to heat tint any pre-existing crack surfaces. The samples were then allowed to cool in still air to ambient temperature. Subsequently, the test weld was fractured open by simple bending, allowing visual examination of fractured surfaces. The fractured faces



Note: All dimensions in millimetres [not to scale].

Figure 3 – Schematic diagram of the G-BOP test block design that allows four weld beads to be deposited on each test block

of all weld deposits were digitally recorded and visually examined at a magnification of 20x. The proportion of discolored transverse crack area, A_C , and total fused metal area, A_F , were precisely measured by using digital image analysis software. From the measured areas, the percentage cracking was then calculated following Equation (1):

$$\text{Percentage cracking} = \frac{A_C}{A_F} \times 100 \quad (1)$$

In addition to the percentage room temperature cracking (RTC), for each set of G-BOP samples, the 10 % crack preheat temperature (10 % CPT) and the critical preheat temperature (CPT) were also determined.

Three welding variables were selected to study their effects on susceptibility to cold cracking, namely: welding current, CTWD and shielding gas. Values used are given in Table 4. The chosen ranges of welding parameters were within the recommended ranges from both wire manufacturers, and reflect the general industrial practice for welding in the downhand position.

Table 4 – Matrix of welding parameters investigated in this current work to determine effect on weld metal diffusible hydrogen content in H5 and H10 weld deposits

| Welding parameter | Testing range |
|--------------------------------------|--|
| Welding current (A) | 280 – 300 – 320 |
| CTWD (mm) | 15 – 20 – 25 |
| Heat input (kJ/mm) | 1.26 – 1.35 – 1.44 |
| Shielding gas (l/min) | 75Ar-25CO ₂ and CO ₂ |
| Welding voltage* (V) | 29 – 30 |
| Travel speed* (mm/min) | 400 |
| Note: * Not investigated parameters. | |

Table 3 – Chemical composition of parent material used for G-BOP test

| | C | Mn | Si | S | P | Ni | Cr | Mo | Cu | V | Nb | Ti | N | Al | CE _{IW} | Pcm |
|-------|------|------|------|-------|-------|-------|-------|-------|-------|-------|-------|-------|--------|-------|------------------|------|
| Check | 0.17 | 1.23 | 0.34 | 0.008 | 0.015 | 0.024 | 0.021 | 0 | 0.01 | 0 | 0 | 0.018 | 0.0015 | 0.029 | 0.38 | 0.24 |
| Ladle | 0.15 | 1.25 | 0.32 | 0.009 | 0.014 | 0.024 | 0.023 | 0.003 | 0.007 | 0.004 | 0.001 | 0.019 | 0.0028 | 0.028 | 0.37 | 0.23 |

4 RESULTS

The results from testing of H10 and H5 weld metals using a range of preheat temperatures are summarised in Tables 5, 6, 7 and 8.

The G-BOP test results for H10 weld metal showed cold cracking for all combinations of welding parameters selected at the no-preheat condition of 20 °C. In contrast, the H5 weld metals exhibited no cracking at room temperature. Therefore, the examination of H5 at higher preheat temperatures was not pursued. The results for percentage cracking as a function of preheat temperature for all conditions investigated in the G-BOP tests are shown graphically in Figure 4.

5 DISCUSSION

5.1 Effect of welding current when using 75Ar-25CO₂ shielding gas

Despite the significant differences in the weld metal hydrogen content across all samples (10.5-17.0 ml/100 g), and largely irrespective of welding current, the percentage room temperature cracking (RTC) for eight out of ten G-BOP samples revealed 100 % cracking. Only two samples welded using the highest welding current of 320 A exhibited lower cracking susceptibility, but only marginally lower than 100 % RTC.

From the diagrams presented in Figure 4 for the H10 weld deposits, it is apparent that the effect of welding current on weld metal cracking under mixed shielding gas depends strongly on other welding parameters, such as CTWD and preheat temperature. In general, increasing current appears to result in a tendency for reduced crack susceptibility, although this effect is much more significant at low CTWD. This is presumably due to the more significant effect of increasing current on reducing H_D at CTWD of 15 mm.

As expected, by introducing preheat temperatures from 50 to 120 °C, the percentage of cold cracking was progressively reduced. At the shortest CTWD of 15 mm (see graph (A15) in Figure 4) the plotted lines for each current level are further apart than those plotted in graphs (A20) or (A25) for CTWDs of 20 and 25 mm, respectively. This effect is probably due to the generally higher and wider range of hydrogen levels for weld metal produced at 15 mm CTWD (13.8-17.0 ml/100 g), compared to the H_D levels at CTWDs of 20 mm (12.9-14.8 ml/100 g) and 25 mm (10.5-12.0 ml/100 g).

It should be noted that the weld metal deposited using the lowest welding current of 280 A at 15 mm CTWD contained the maximum amount of diffusible hydrogen (17.0 ml/100g) and also exhibited a significantly higher percentage of cracking up to the preheat temperature of 80 °C. This observation confirms an expectation from the earlier work that an increase in welding current reduces the weld metal diffusible hydrogen levels [12], and therefore a current increase would be expected to reduce susceptibility to cold cracking for 75Ar-25CO₂ shielding gas and a CTWD of 15 mm.

5.2 Effect of welding current when using CO₂ shielding gas

The percentage cracking observed when using CO₂ shielding gas showed a more complex relationship with welding current, particularly at the shortest CTWD of 15 mm. The increase of welding current, which resulted in a slight (perhaps insignificant) increase of weld metal diffusible hydrogen content, produced a significant and unexpected reduction of susceptibility to cold cracking at room temperature, as shown in diagram (C15) of Figure 4. This effect was also observed when preheating was employed. Possible explanations for this phenomenon are the geometry of the G-BOP welds cross sections, as shown in Figure 5, or differences in weld metal microstructure and mechanical properties. The

Table 5 – Percentage of cracking for H10 welds deposited using 75Ar-25CO₂ shielding gas

| Welding parameters | | | Preheat temperature (°C) | | | | | H _D (ml/100 g) |
|------------------------|-----------------------------|--------------|----------------------------|-----|----|-----|-----|------------------------------|
| | | | 20 | 50 | 80 | 100 | 120 | |
| Welding current (A) | Shielding gas (18 l/min) | CTWD (mm) | Percentage cracking (%) | | | | | |
| 280 | 75Ar-25CO ₂ | 15 | 100 | 100 | 88 | 0 | - | 17.0 |
| 280 | | 20 | 100 | 98 | 16 | 18 | 0 | 14.8 |
| 280 | | 25 | 100 | 100 | 29 | 0 | - | 12.0 |
| 300 | | 15 | 100 | 96 | 39 | 17 | 0 | 14.3 |
| 300 | | 20 | 100 | 100 | 53 | 11 | 0 | 12.9 |
| 300 | | 25 | 100 | 100 | 31 | 0 | - | 11.0 |
| 320 | | 15 | 97 | 70 | 18 | 0 | - | 13.8 |
| 320 | | 20 | 100 | 82 | 36 | 4 | - | 13.1 |
| 320 | | 25 | 94 | 83 | 30 | 0 | - | 10.5 |
| RH (%): | | | 50 | 37 | 45 | 28 | 44 | |
| Temperature (°C): | | | 17 | 18 | 25 | 26 | 22 | |

Table 6 – Percentage of cracking for H10 welds deposited using CO₂ shielding gas

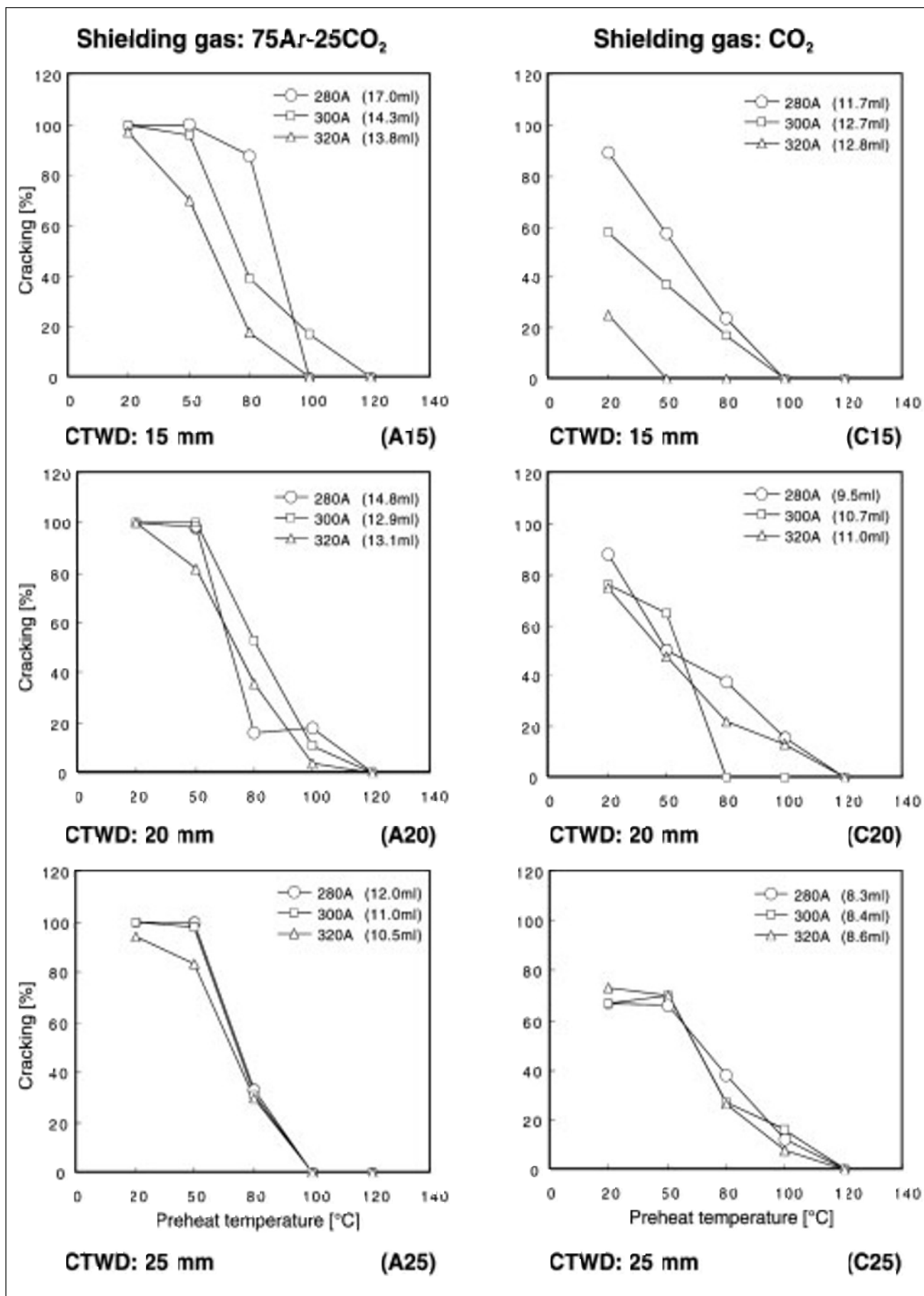
| Welding parameters | | | Preheat temperature (°C) | | | | | H _D (ml/100 g) |
|------------------------|-----------------------------|--------------|----------------------------|----|----|-----|-----|------------------------------|
| Welding current (A) | Shielding gas (18 l/min) | CTWD (mm) | 20 | 50 | 80 | 100 | 120 | |
| | | | Percentage cracking (%) | | | | | |
| 280 | CO ₂ | 15 | 89 | 57 | 24 | 0 | - | 11.7 |
| 280 | | 20 | 88 | 50 | 38 | 16 | 0 | 9.5 |
| 280 | | 25 | 67 | 66 | 38 | 12 | 0 | 8.3 |
| 300 | | 15 | 58 | 37 | 17 | 0 | - | 12.7 |
| 300 | | 20 | 76 | 65 | 0 | 0 | - | 10.7 |
| 300 | | 25 | 67 | 70 | 27 | 16 | 0 | 8.4 |
| 320 | | 15 | 25 | 0 | 0 | 0 | - | 12.8 |
| 320 | | 20 | 75 | 48 | 22 | 13 | 0 | 11.0 |
| 320 | | 25 | 73 | 70 | 26 | 8 | 0 | 8.6 |
| RH (%): | | | 44 | 44 | 45 | 42 | 44 | |
| Temperature (°C): | | | 22 | 22 | 25 | 26 | 22 | |

Table 7 – Percentage of cracking for H5 welds deposited using 75Ar-25CO₂ shielding gas

| Welding parameters | | | Preheat temperature (°C) | | | | | H _D (ml/100 g) |
|------------------------|-----------------------------|--------------|----------------------------|----|----|-----|-----|------------------------------|
| Welding current (A) | Shielding gas (18 l/min) | CTWD (mm) | 20 | 50 | 80 | 100 | 120 | |
| | | | Percentage cracking (%) | | | | | |
| 280 | 75Ar-25CO ₂ | 15 | 0 | - | - | - | - | 3.5 |
| 280 | | 20 | 0 | - | - | - | - | 2.2 |
| 280 | | 25 | 0 | - | - | - | - | 1.5 |
| 300 | | 15 | 0 | - | - | - | - | 3.1 |
| 300 | | 20 | 0 | - | - | - | - | 2.1 |
| 300 | | 25 | 0 | - | - | - | - | 1.7 |
| 320 | | 15 | 0 | - | - | - | - | 2.6 |
| 320 | | 20 | 0 | - | - | - | - | 1.6 |
| 320 | | 25 | 0 | - | - | - | - | 1.6 |
| RH (%): | | | 42 | - | - | - | - | |
| Temperature (°C): | | | 17 | | | | | |

Table 8 – Percentage of cracking for H5 welds deposited using CO₂ shielding gas

| Welding parameters | | | Preheat temperature (°C) | | | | | H _D (ml/100 g) |
|------------------------|-----------------------------|--------------|----------------------------|----|----|-----|-----|------------------------------|
| Welding current (A) | Shielding gas (18 l/min) | CTWD (mm) | 20 | 50 | 80 | 100 | 120 | |
| | | | Percentage cracking (%) | | | | | |
| 280 | CO ₂ | 15 | 0 | - | - | - | - | 1.9 |
| 280 | | 20 | 0 | - | - | - | - | 1.8 |
| 280 | | 25 | 0 | - | - | - | - | 1.1 |
| 300 | | 15 | 0 | - | - | - | - | 1.5 |
| 300 | | 20 | 0 | - | - | - | - | 1.3 |
| 300 | | 25 | 0 | - | - | - | - | 0.9 |
| 320 | | 15 | 0 | - | - | - | - | 1.7 |
| 320 | | 20 | 0 | - | - | - | - | 1.5 |
| 320 | | 25 | 0 | - | - | - | - | 0.9 |
| RH (%): | | | 42 | - | - | - | - | |
| Temperature (°C): | | | 17 | | | | | |



Diffusible hydrogen contents are shown in parentheses for each welding current.

Figure 4 – Graphs showing the percentage cracking for H10 weld metal in G-BOP tests using 75Ar-25CO₂ and CO₂ shielding gases at welding currents 280, 300 and 320 A and CTWD of 15, 20 and 25 mm

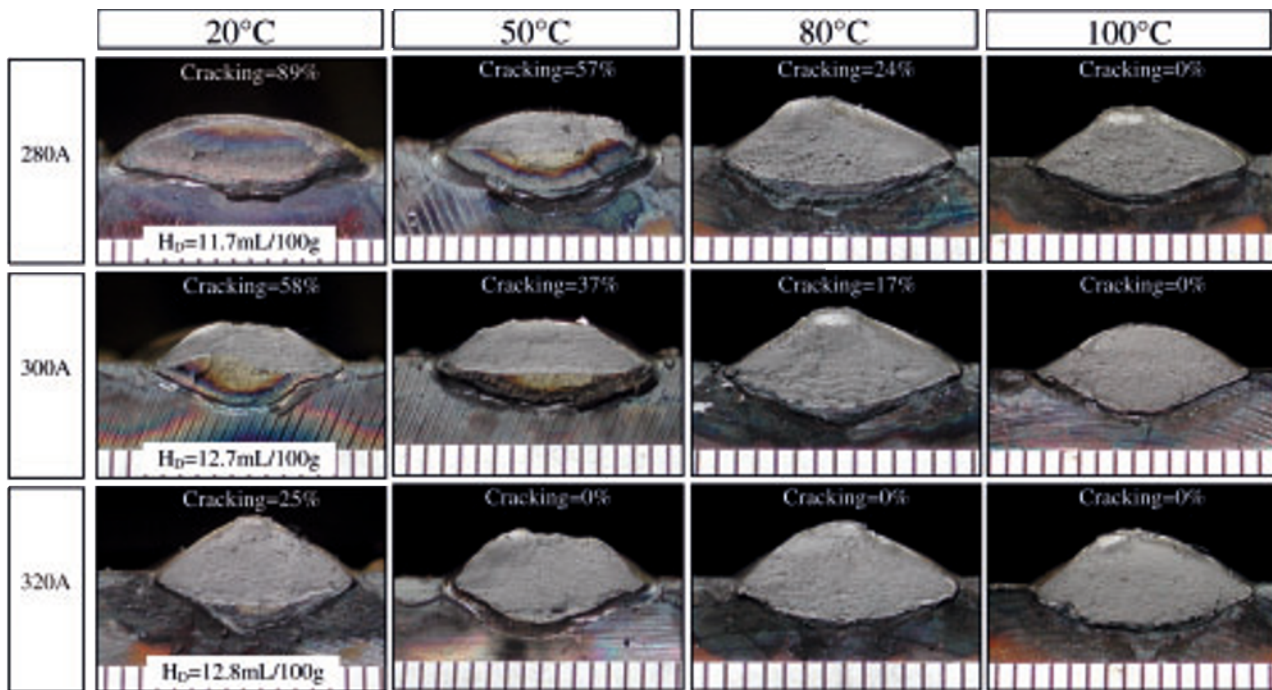


Figure 5 – Photographs showing the G-BOP fracture surfaces with cracking percentage of H10 weld metal deposited with preheats of 20, 50, 80 and 100 °C using CO₂ shielding gas and CTWD of 15 mm

fused weld metal profiles varied significantly with welding current increase at the 20 °C preheat. For example, the weld deposited using the lowest welding current of 280 A was characterised by a very flat and wide bead profile (89 % RTC), whereas the sample welded using high welding current of 320 A was characterised by deeper penetration and a higher bead height, and it showed only 25 % RTC. Increase in preheat temperature appears to suppress this bead shape effect and the weld deposit contours gradually become more uniform. This change in bead profile appears to correlate well with the observed RTC results.

Although the diffusible hydrogen range for 15 mm CTWD is relatively narrow in this case of CO₂ shielding gas (11.7-12.8 ml/100 g), an increase in welding current was found to be beneficial, significantly reducing the weld metal cold cracking susceptibility at all preheat temperatures examined in this work. At the lowest CTWD of 15 mm the welding current appears to be the governing variable in reduction of cracking percentage at 20, 50 and 80 °C preheat temperature, rather than H_D. However, for an increase of CTWD from 15 to 25 mm, the weld metals contain lower hydrogen levels and a narrower range of diffusible hydrogen contents (8.3-8.6 ml/100 g). In this case, a change in welding current has a less significant effect, as illustrated by graph (C25) in Figure 4.

5.3 Effect of CTWD

The effect of an increase in CTWD from 15 to 25 mm on cracking susceptibility is best illustrated in Figure 4, which shows that the relationship between the CTWD and percentage weld metal cracking results is ambiguous. Although the CTWD appears to be a significant variable

in the hydrogen content, its effect on weld metal hydrogen cracking varied depending on the shielding gas used. Regardless of weld metal diffusible hydrogen levels at ambient temperature, the CTWD increase had no effect on percentage of RTC at this temperature when welding involved 75Ar-25CO₂ shielding gas. The majority of G-BOP samples exhibited close to 100 % RTC. However, when using CO₂ shielding gas the weld metal cracking was found to be more complex, as shown in diagrams (C15), (C20) and (C25) of Figure 4. Interestingly, at a CTWD of 15 mm using CO₂ shielding gas there appears to be a large scatter in RTC caused by variation in welding current. It should be noted that the weld metal hydrogen levels varied marginally (11.7-12.8 ml/100 g), but by increasing welding current the percentage of RTC decreased from 89 to 25 %. By increasing of preheat temperature to 50, 80 and 100 °C, the variation of the % cracking parameter was gradually narrowed [see Figure 4, (C15)]. The bead deposited with no preheat at 15 mm CTWD and a welding current of 320 A, contained the highest level of diffusible hydrogen (12.8 ml/100 g) yet exhibited the smallest of RTC of 25 %.

Although it is generally recognised that increasing CTWD significantly reduces weld metal diffusible hydrogen, the results indicate that the lowest value of RTC occurred in weld metal containing the highest diffusible hydrogen content in the range between 11.7 -12.8 ml/100g for a CTWD of 15 mm and CO₂ shielding gas [see Figure 4, (C15)]. Despite the smallest diffusible hydrogen range (8.3- 8.6 ml/100 g) for welds deposited using a CTWD of 25 mm and CO₂ shielding gas [see Figure 4, (C25)], increasing the preheat temperature was not as effective in reducing % cracking as for welds deposited using CTWD of 15 mm and the same shielding gas. It is therefore once again proposed that H_D may not be the

most important factor in all cases, and that other factors such as weld bead profile and weld metal mechanical properties (for example, hardness) may also be influential.

5.4 Effect of shielding gas

The investigation revealed that the shielding gas affects the susceptibility of weld metal to transverse cold cracking, as shown by the results for the various preheat temperatures presented in Figure 6. The results are intuitive in relation to the previous work showing the shielding gas effects on diffusible hydrogen levels [12]. For constant CTWD and welding current, the weld metal deposited using the mixed 75Ar-25CO₂ shielding gas generally exhibited a larger percentage of cracking than for the CO₂ shielding gas at room temperature. At preheat temperatures of 50 and 80 °C, the decrease of percentage of cracking was more noticeable under CO₂ shielding gas at a CTWD of 15 mm, as shown in Figure 6 a). However, further increase of preheat temperature from 80 and 100 °C resulted in a significant decrease in weld metal cracking for mixed shielding gas. Despite the fact that the percentage cracking values were significantly lower for CO₂ shielding gas for all G-BOP samples, the critical preheat temperatures for no cracking were found to be similar for both shielding gases.

A different relationship between percentage cracking and shielding gas was observed at CTWD of 25 mm, shown in Figure 6 b). At room temperature and 50 °C preheat conditions, the weld metal deposited using CO₂ shielding gas was characterised by significantly less cracking (67 % RTC) compared with the 75Ar-25CO₂ deposit (100 %). However, a more rapid decrease in percentage of cracking was observed as preheat temperature was increased from 50 and 80 °C on welds deposited using the 75Ar-25CO₂ shielding gas. This

steeper reduction of cracking percentage in samples welded using mixed gas resulted in no cracking at 100 °C, whereas in CO₂ shielding gas the cracking was present until the preheat temperature reached 120 °C.

The effect of weld metal diffusible hydrogen content on cracking susceptibility at room temperature for 75Ar-25CO₂ and CO₂ shielding gas deposits is shown in Figure 7. It is apparent that CO₂ shielding gas deposits exhibited generally lower RTC values than 75Ar-25CO₂ weld deposits at similar levels of diffusible hydrogen. Although the ranges of hydrogen levels only partly overlap, the percentage cracking at room temperature was significantly lower in welds deposited using CO₂ shielding gas. This finding not only illustrates the differences in diffusible hydrogen generated in weld metal by the two shielding gases, but also demonstrates that the weld metals have different sensitivities to cold cracking. The two points residing outside of the expected band represent welds with bead contours that are noticeably different to other weld beads. The diffusible hydrogen contents for the three beads identified in Figure 7 were similar in range (11.7 to 12.8 ml/100 g), but the amount of percentage cracking at room temperature varied significantly. These differences may be due to the marked differences in the weld profiles, illustrated by the macrographs included in the figure. It is important to note, that by increasing preheat temperature, the samples welded using 75Ar-25CO₂ exhibited a steeper reduction of percentage of cracking than the CO₂ weld deposits, especially in samples welded using a CTWD of 25 mm [see Figure 4, (A25) and (C25)].

5.5 RTC vs 10 % CPT

The effect of increase in preheat temperature on the reduction of cracking can be expressed by the 10 % CPT value. This parameter is particularly useful when the weld metal containing higher hydrogen levels gives 100 % RTC.

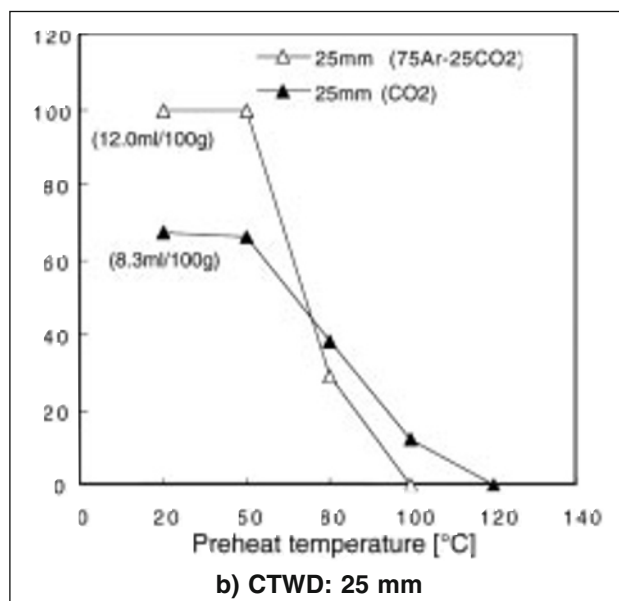
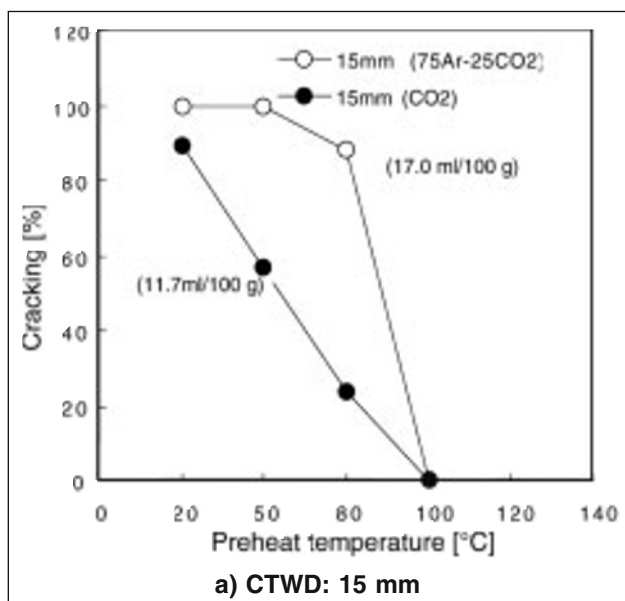


Figure 6 – Graphs showing the percentage cracking for H10 weld metal in G-BOP tests, using 75Ar-25CO₂ and CO₂ shielding gases, constant welding current 280 A

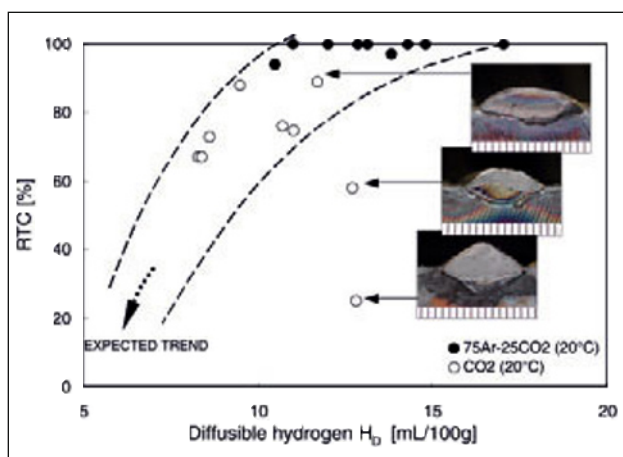


Figure 7 – Graph showing the percentage cracking for room temperature welding using H10 weld metal, 75Ar-25CO₂ and CO₂ shielding gases, welding currents of 280, 300 and 320 A and CTWD values of 15, 20 and 25 mm

The H10 welds deposited using the 75Ar-25CO₂ shielding gas, characterised by higher diffusible hydrogen levels, display a higher cracking susceptibility at room temperature compared to those deposited using CO₂ shielding gas. However, as illustrated in Figure 8, the welds deposited using 75Ar-25CO₂ and CO₂ shielding gases revealed similar values of 10 % CPT in the range 95-110 °C. This finding demonstrates that although the welds deposited using CO₂ shielding gas exhibited a higher resistance to cold cracking to those deposited using 75Ar-25CO₂ shielding gas at room temperature, both types of welds showed a similar response to pre-heat. The generally higher hydrogen levels in the 75Ar-25CO₂ welds did not appear to affect the 10 % CPT value. Note that the outlying point in Figure 8 (arrowed), represents a weld sample with bead contour different to the other weld beads, as discussed earlier. This sample not only exhibited the smallest 10 % CPT value of 40 °C, but also the lowest amount of cold cracking at room temperature (25 % RTC). It is concluded that this result is an anomaly resulting from an unusual bead geometry.

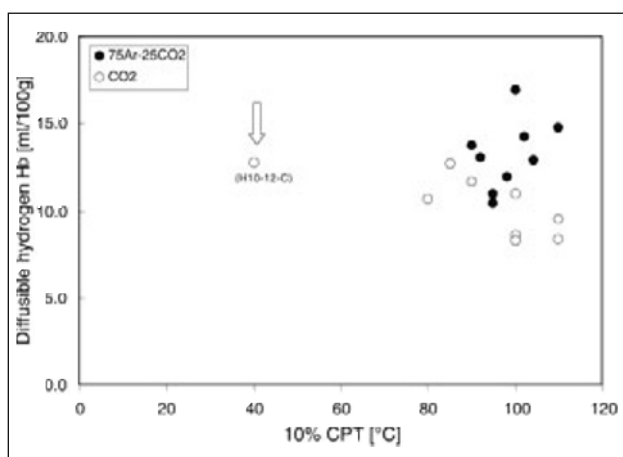


Figure 8 – Graph showing the relationship between 10 % CPT and diffusible hydrogen levels for G-BOP welds deposited using H10 wires, welded using 75Ar-25CO₂ and CO₂ shielding gases

It is therefore concluded that although welds deposited using 75Ar-25CO₂ may exhibit a higher degree of cracking at room temperature, this does not necessarily mean that the weld will require significantly higher preheat temperature to eradicate cracking.

5.6 Weld metal hardness

Samples of welds from the G-BOP tests were extracted for Vickers micro-hardness measurements using 0.5 kg load from both H10 and H5 weld deposits. The hardness values reported are averages determined from a minimum of five measurements. Since the G-BOP samples of H5 weld metal exhibited no cracking at room temperature and no welding was carried out at higher preheat temperatures, the effects of increasing preheat temperatures on H5 weld deposit hardness could not be presented here.

In the no preheat condition, the welds deposited using 75Ar-25CO₂ revealed higher hardness values than deposited with corresponding wires under CO₂ shielding gas, as shown in Figure 9 for welds deposited at a welding current of 300 A and a CTWD of 25 mm for both the H5 and H10 wires. Both welding consumables exhibited a similar hardness increase (20 HV_{0.5}) due to a change from CO₂ to 75Ar-25CO₂ shielding gas.

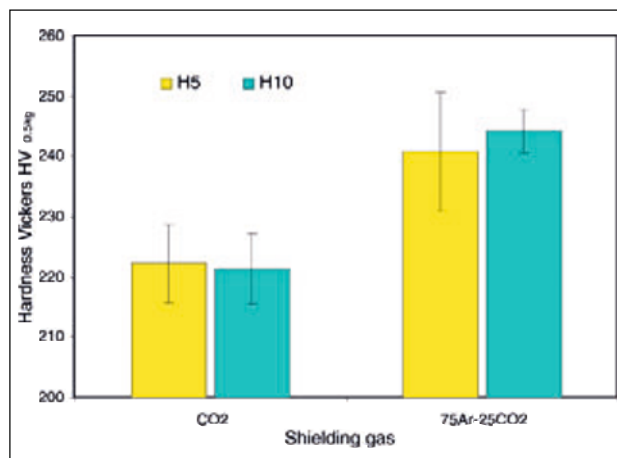


Figure 9 – A plot of hardness values for G-BOP welds deposited using H5 and H10 wires both welded at ambient temperature with welding current of 300 A, CTWD of 25 mm and the two shielding gases

The relationships between the welding current and hardness values for H10 welds deposited at the preheat temperature of 20 °C, and a CTWD of 25 mm are shown in Figure 10 for both shielding gases. The weld metal hardness was found to increase with increasing welding current using CO₂ shielding gas (an increase in welding current from 280 to 320 A resulted in an increase of weld metal hardness from 215 to 233 HV_{0.5}). However, the weld metal hardness remained unchanged in welds deposited using 75Ar-25CO₂ shielding gas. It is inferred that increasing welding current for CO₂ welding changes the microstructure and/or composition, whereas mixed gas welding does not. Further investigation is required

to clarify this difference, however, it is clear that the increase in hardness with increasing current does not appear to have a significant effect on the percentage cracking observed, as shown in Figure 4, graph (C25). Since a similar effect might be expected at the CTWD of 15 mm, it is suggested that the difference in weld bead profile is most likely responsible for the observed difference in RTC under CO₂ at CTWD of 15 mm.

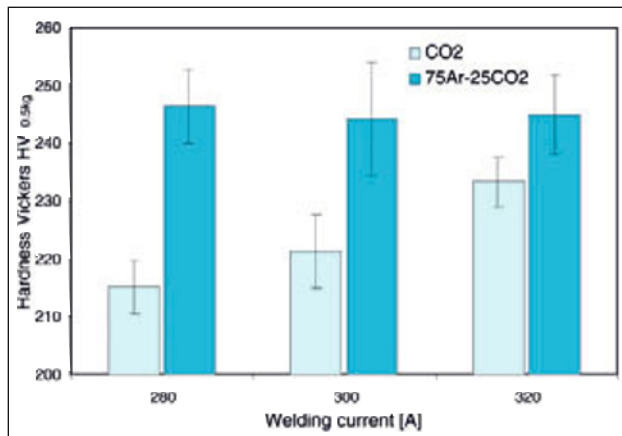


Figure 10 – A plot of hardness values for G-BOP welds deposited using the H10 wire at various welding currents (280, 300 and 320 A) using CO₂ and 75Ar-25CO₂ shielding gases, CTWD of 25 mm and preheat temperature of 20 °C

A gradual decrease of weld metal hardness with increasing preheat temperature was observed, as shown in Figure 11. The samples welded using 75Ar-25CO₂ exhibited a greater reduction of hardness with increasing preheat temperature than those welded using CO₂ shielding gas. For example, the hardness decreases for an increase in preheat temperature from 20 to 120 °C, were 22 and 7 Vickers hardness points for 75Ar-25CO₂ and CO₂ shielding gas, respectively.

The lower decrease in hardness for CO₂ shielding gas is possibly related to the leaner chemistry of the welds as a result of the higher oxidizing potential of the shield-

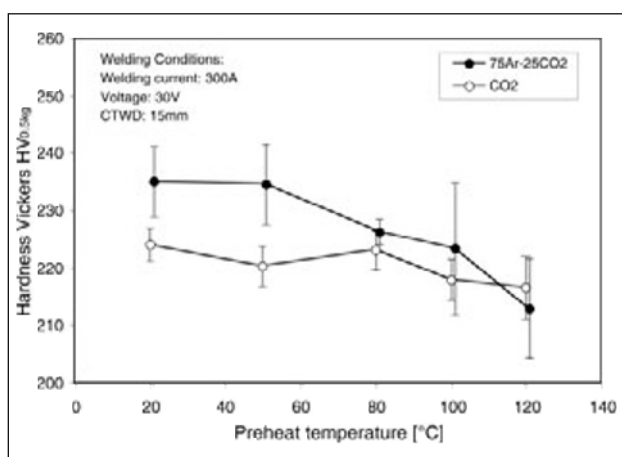


Figure 11 – A plot of hardness values for G-BOP weld deposited using H10 wire at various preheat temperatures and using 75Ar-25CO₂ and CO₂ shielding gas

ing atmosphere. This is likely to have resulted in reduced recovery of alloying elements such as Mn, Si and B. While CE_{IW} values are very similar for both the H5 and H10 wires, the Pcm values for the H10 wire samples were noticeably higher for both shielding gases used. This is due to higher levels of carbon and boron in the H10 weld metal deposits, since both carbon and boron concentration are more important factors in the Pcm carbon equivalent formula. A graphical comparison of the carbon equivalent values is presented in Figure 2. It should be noted that the CE_{IW} and Pcm values were calculated from multiple layer “all-weld metal” deposits and different values would be obtained from a single weld bead due to the dilution effects. Typically, the use of CO₂ shielding gas reduces Mn, Si and B recovery, and this has resulted in marginally lower CE_{IW} and Pcm values for both consumables. Further, the higher as welded hardness of the more highly alloyed 75Ar-25CO₂ welds is more markedly affected by increasing preheat because of structural coarsening due to the lower weld cooling rate.

In summary, weld metal hardness was found to be reduced by an increase in preheat temperature for both shielding gases, although the effect was more pronounced for the mixed gas. The results of weld metal hardness measurements confirmed a consistent difference in weld metal hardness for both welds deposited using different shielding gases.

6 CONCLUSIONS

This paper reports the findings of an investigation into the effects of welding parameters and shielding gases on HACC susceptibility of weld metal deposited by seamless (H5) and seamed (H10) rutile wires. The major conclusions drawn from this investigation are as follows:

- (1) E71-T1 (rutile) weld metal containing diffusible hydrogen of ≥ 10 ml/100 g is highly susceptible to cold cracking at room temperature in the G-BOP test.
- (2) In contrast, the H5 weld deposits (< 5 ml/100 g) exhibited no cracking in the G-BOP test at room temperature under any welding conditions investigated.
- (3) The G-BOP test results indicate that although the same welding consumable (H10) deposited using different shielding gases can show different responses to preheat temperature, a preheat temperature of 120 °C decreases cracking to ≤ 10 % for welds deposited using both shielding gases.
- (4) The results of room temperature G-BOP tests show that the susceptibility of weld metal to HACC is reduced in welds deposited using CO₂ shielding gas for all combinations of CTWD and welding current investigated. This effect is largely due to the lower levels of diffusible hydrogen in welds deposited using CO₂.
- (5) Increasing preheat was found to decrease the percentage of cracking in the H10 weld deposits in all cases. A major effect of increasing preheat temperature is to decrease the diffusible hydrogen concentration.

(6) An increase in preheat temperature from 20 to 120 °C reduced the weld metal hardness by 22 and 7 points HV0.5 for welds deposited using 75Ar-25CO₂ and CO₂ shielding gas, respectively. The role of such a reduction in hardness on cracking susceptibility is not clear, but it is not likely to be significant on the basis of current results.

(7) For test welds deposited at 20 °C, using 75Ar-25CO₂ shielding gas and a CTWD of 15 mm, an increase in the welding current was found to reduce the weld metal diffusible hydrogen levels, but not the susceptibility to cold cracking. In the case of the G-BOP tests welds deposited under CO₂ shielding gas, an increasing welding current resulted in a significant reduction of cold cracking at room temperature at a CTWD of 15 mm, despite a slight increase in H_D. This effect was most likely due to variation in weld bead geometry, rather than differences in H_D or weld metal hardness.

(8) Shielding gas composition influenced the chemical composition of the weld deposits. For both welding consumables (H10 and H5), welds deposited using 75Ar-25CO₂ shielding gas exhibited higher CE_{IW} and Pcm values than the weld metal deposited using CO₂ shielding gas. This compositional difference is consistent with the observed hardness trends of the welds. The measured hardness results for welds produced with the same weld metals parameters were about 20 HV0.5 points higher for 75Ar-25CO₂ compared to those deposited using CO₂.

ACKNOWLEDGEMENTS

This work was conducted as part of a project sponsored by the CRC for Welded Structures (CRC-WS), established by the Australian Government Co-operative Research Centres Program. The work presented in this paper was also supported by the Welding Technology Institute of Australia (WTIA) Technical Panel 2 Working Group members, including Blue Scope Steel Ltd, Defence Science and Technology Organisation and University of Wollongong (UOW). The authors would like to especially acknowledge Welding Industries of Australia and CIGWELD Thermadyne for provision of the welding consumables and laboratories. The authors are also grateful to Prof. D.P. Dunne from UOW for his valuable comments. It should be noted that the present work has been published in similar form in the Australasian Welding Journal, and copyright permission has kindly been extended by WTIA.

REFERENCES

- [1] Kinsey A.J.: The welding of structural steels without preheat, *Welding Journal*, April 2000, pp. 79-88s.
- [2] Jones A.R., Hart P.H.M.: Improving procedure prediction to avoid hydrogen cracking when welding C-Mn steels, TWI Report 225, October 1983.
- [3] AS/NZS 1554.1-2000: Structural steel welding – Welding of steel structures, Standards Australia, 2000.
- [4] AS/NZS 1554.4-1995: Structural steel welding – Welding of high strength quenched and tempered steels, Standards Australia, 1995.
- [5] AWS D1.1-2000: Structural welding code – steel, AWS, 2000.
- [6] EN 1011-2-2001: Welding – Recommendations for welding of metallic materials – Arc welding of ferritic steels, 2001.
- [7] Uwer D., Hohne H.: Characterisation of the cold cracking behaviour of steels during welding, *Welding and Cutting*, 1991, Vol. 43, 4, pp. 195-199.
- [8] Hart P.H.M.: Hydrogen cracking – its cause, costs and future occurrence, Proc. of the 1st International Conference on Weld Metal Hydrogen Cracking in Pipeline Girth Welds, Publ. by WTIA, Wollongong, March 1999. p. 3-1.
- [9] Yurioka N., Suzuki H.: Hydrogen assisted cracking in C-Mn and low alloy steel weldments, *International Materials Reviews*, 1990, Vol. 35, No. 4, pp. 217-249.
- [10] Kuebler R., Pitrun M., Pitrun I.: The effect of welding parameters and hydrogen levels on the weldability of high strength Q&T steel welded with FCAW consumables, *Australasian Welding Journal*, 1st Quarter, 2000, Vol. 45, pp. 38-47.
- [11] Visman V.: Weld metal HACc in thick section, low strength multi-pass FCAW, Honours Thesis, University of Wollongong, Australia, 2002.
- [12] Pitrun M., Nolan D., Dunne D.: Diffusible hydrogen content in rutile flux-cored arc welds as a function of the welding parameters, Doc. IIW-1615-03 (ex. Doc. IX-2064-03), *Welding in the World*, 2004, Vol. 48, No. 1/2, pp. 2-13.
- [13] Reeve L.: A summary of reports of investigations on selected types of high strength steels, *Trans. Inst. Welding*, April 1940, pp. 177-202.
- [14] Hoffmeister H., Matthia A.: The effects of test conditions on hydrogen assisted weld cracking of StE 355, StE 465, StE 690 high strength steels, IIW Doc. No. IX-1621-90, 1990.
- [15] Davidson J.L.: Hydrogen-induced cracking of low carbon – Low alloy steel weldments, *Material Forum*, 1995, 19, pp. 35-76.
- [16] Graville B.A.: Interpretive report on weldability tests for hydrogen cracking of higher strength steels and their potential for standardization, *Welding Research Council, Bulletin 400*, April 1995.
- [17] API Recommended Practice 4009, April 1977.
- [18] BS 7363-1990: Methods for controlled thermal severity (CTS) test and bead-on-plate (BOP) test for welds, 1990.
- [19] NF A89-100: 1991: Welding and allied processes – Cold cracking on implants – Test method, 1991.
- [20] JIS Z3158-1996: Method of Y-groove cracking test, 1996.
- [21] Seferian D.: *The Metallurgy of Welding*, Chapman and Hall, London, 1962.
- [22] Makara A.M.: Cold transverse cracks in low-alloy high strength welds, *Avtomaticeskaja Svarka*, 1971, Vol. 11, pp. 1-4.

- [23] Graville B.A., McParlan M.: Weld metal cold cracking, *Metal Construction and British Welding Journal*, February 1974, pp. 62-63.
- [24] McParlan M., Graville B.A.: Hydrogen cracking in weld metals, *Welding Journal*, April 1976, pp. 95-102s.
- [25] Chakravarti A.P., Balsa S.R.: Evaluation of weld metal cold cracking using the G-BOP test, *Welding Journal*, January 1998, pp. 1-8s.
- [26] Hart P.H.M.: Resistance to hydrogen cracking in steel weld metals, *Welding Journal*, January 1986, pp. 14-22s.
- [27] Atkin G., Thiessen D., Nissley N., Adonyi Y.: Welding process effects in weldability testing of steels, *Welding Journal*, April 2002, pp. 61-68s.
- [28] Lazor R.B., Graville B.A.: Effect of microalloying on weld cracking in low carbon steels, *Canadian Welder and Fabricator*, July 1983, Vol. 74, pp. 21-23.
- [29] Chen L.: Characterisation of transverse cold cracking in weld metal of a high strength quenched and tempered steel, PhD Thesis, University of Wollongong, 1999.
- [30] ANSI/AWS A5.20-95: Specification for carbon steel electrodes for flux cored arc welding, 1995.
- [31] AS 2203.1-1990: Cored electrodes for arc welding – Ferritic steel electrodes, Standards Australia, 1990.
- [32] ISO 3690: 2000: Welding and allied processes – Determination of hydrogen content in ferritic steel arc weld metal, 2000.